

## The effect of interfacial morphology on the magnetic and magnetocaloric properties of ferromagnetic nanoparticles with core-shell geometry: a Monte Carlo Study

Yusuf YÜKSEL\*

Department of Physics, Dokuz Eylül University, İzmir, Turkey

Received: 26.09.2021 • Accepted/Published Online: 22.02.2022 • Final Version: 28.02.2022

**Abstract:** Within the framework of Monte Carlo simulations, we investigate the magnetic and magnetocaloric properties of a nanocomposite particle composed of ferromagnetic core and shell layers. We found that isothermal magnetic entropy change may exhibit two peaks associated to two different phase transitions of the core and shell layers. We paid particular attention to the microscopic details of the core/shell interface. Our results suggest that for the large values of the interface exchange coupling, the full width at half maximum is expanded at the expense of the low temperature peak of isothermal entropy change  $|\Delta S_M|$  whereas the high temperature peak is found to be more or less insensitive to varying exchange coupling. Besides, our simulations yield that magnetocaloric properties of the particles with a cubic core are enhanced in comparison with those composed of truncated cuboctahedral, spherical, octahedral, and asteroid shaped cores.

**Keywords:** Critical behavior, magnetism, Monte Carlo, magnetocaloric effect, nanoparticle

### 1. Introduction

In recent years, investigations of magnetocaloric properties of a variety of magnetic compounds and composite materials have attracted glowing interest in theoretical and experimental research [1]. The magnetocaloric effect (MCE) is a phenomenon in which a magnetic material's temperature can be greatly enhanced by applying a magnetic field under adiabatic conditions. The removal of the field, on the other hand, produces a negative change in the sample's temperature. In order to quantify the magnetocaloric performance of a magnetic material, one can utilize some important figures of merit such as adiabatic temperature change  $\Delta T_{ad}$ , isothermal magnetic entropy variation  $\Delta S_M$ , and refrigerant capacity (RC) which can be calculated using the following relations [2, 3]:

$$\Delta T_{ad} = - \int \frac{T}{C} \left( \frac{\partial M}{\partial T} \right)_T dh, \quad (1)$$

$$\Delta S_M = - \int \left( \frac{\partial M}{\partial T} \right)_T dh, \quad (2)$$

$$RC = - \int_{T_1}^{T_2} \Delta S_M(T)_h dT. \quad (3)$$

\*Correspondence: yusuf.yuksel@deu.edu.tr

In above equations,  $C$  denotes the total heat capacity including the magnetic, lattice, and electronic contributions,  $T$  is the temperature,  $h$  stands for the applied field strength, and  $M$  is the spontaneous magnetization. RC basically measures how much heat is transferred between the cold  $T_1$  and hot  $T_2$  ends of the refrigerant material. Based on the above equations, the materials exhibiting broadened entropy versus temperature curves and enhanced maximum entropy change near room temperature are regarded as promising candidates for technological applications. In this regard, elementary Gd exhibits a temperature variation of  $\Delta T_{ad} = 14.3$  K in the presence of fields such as 7 T [4]. Besides, it exhibits  $\Delta S_M = 10$  J/kg.K with magnetic field variation from 0 to 5 T [5]. With these properties, Gd is the best known magnetocaloric element with enhanced refrigerant properties around its room temperature Curie point. However, from a commercial point of view, since it is a rare earth element, its resource efficiency does not fulfill the requirements as a raw material to be used in active magnetic refrigeration appliances. Hence, seeking new materials exhibiting large  $\Delta S_M$  and RC values in the vicinity of room temperature is a vital task. In order to overcome this point, composite materials exhibiting two or more phases can be synthesized to improve the MCE properties defined in Eqs. (1)–(3).

From the experimental point of view, a number of magnetic composite materials exhibiting multipeak  $\Delta S_M$  versus temperature curves were synthesized by researchers all around the globe [6–11]. A double-peak structure in the same curves was also theoretically predicted for magnetic bilayers [12]. In a conventional ferromagnet, reference temperatures arising in Eq. (3), i.e. the upper and the lower bounds of the temperature range correspond to the temperatures at which  $\Delta S_M = 0.5\Delta S_m^{max}$  with  $\delta T_{FWHM} = T_2 - T_1$  is called the full width at half maximum (Figure 1a). In case of multiphase composites,  $T_1$  and  $T_2$  in Eq. (3) correspond to lower bound of low temperature peak and higher bound of the high temperature peak, respectively (Figure 1b) [9, 13]. In order to expand  $\delta T$  and RC, considerable research activity is also currently devoted by several research groups using various methods, including nanostructuring and developing nanocomposites [13]. For instance, Franco and coworkers [14] investigated the field dependence of Co, Co-Ag, and Ni-Ag core-shell nanoparticles. Gorria et al. [15] found that the full width at half maximum for ball-milled  $\text{Pr}_2\text{Fe}_{17}$  nanoparticles is 60% greater than that of the bulk alloy. Similarly, Hueso and colleagues [16] showed that MCE in  $\text{La}_{0.67}\text{Ca}_{0.33}\text{MnO}_{3-\delta}$  nanoparticles can be experimentally tuned by means of the particle size.

In the present work, we introduce a model to simulate the magnetocaloric properties of a three-dimensional composite nanoparticle with core/shell morphology exhibiting multipeak  $\Delta S_M(T)$  curves. Particular emphasis is placed on the influence of the interfacial interactions and interface morphology. For this aim, the paper is organized as follows: In Section 2, we introduce our model and simulation details. Our numerical results and related discussions are given in Section 3. Finally, Section 4 is devoted to our conclusions.

## 2. Model and formulation

We consider a three dimensional, ferromagnetic nanoparticle composed of a core which is surrounded by a shell layer (see Figure 2). The Hamiltonian defining our model can be written as

$$\mathcal{H} = -J_c \sum_{\langle i,j \rangle} S_i S_j - J_{sh} \sum_{\langle k,l \rangle} S_k S_l - J_{int} \sum_{\langle i,k \rangle} S_i S_k - h \sum_n S_n, \quad (4)$$

where  $S_i = \pm 1$  is a pseudo spin variable which resides on the nodes of a simple cubic lattice. The first term represents the interactions between the magnetic moments located at the particle core. The

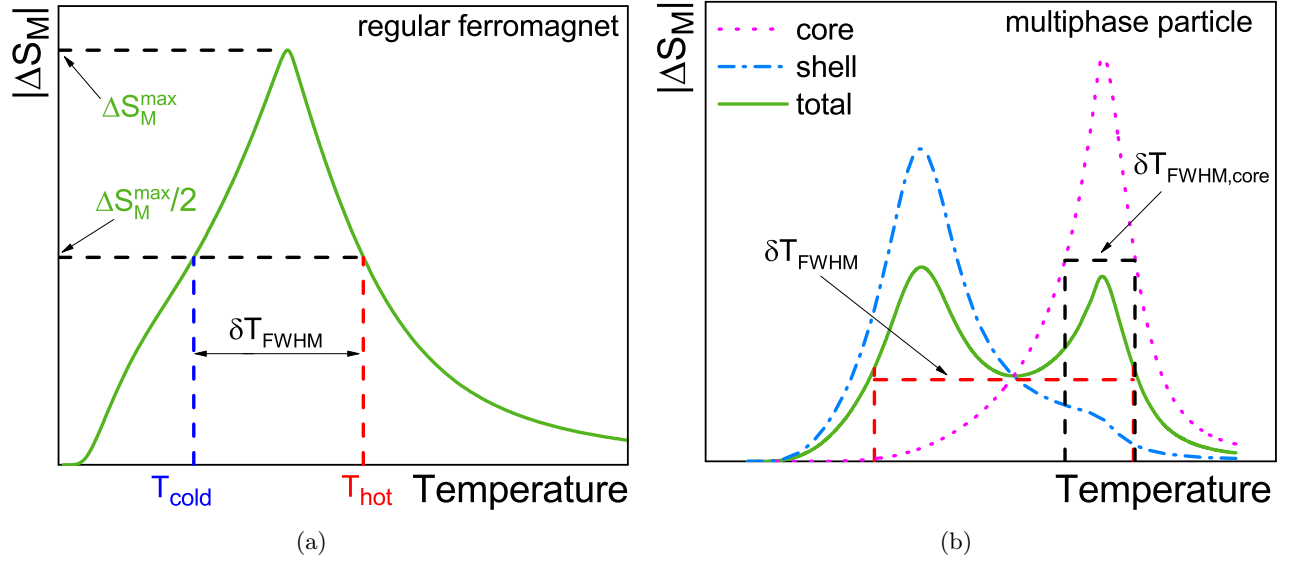


**Figure 1.** Schematic illustration of variation of magnetic entropy change as a function of temperature for (a) single phase ferromagnets, (b) composite ferromagnets composed of two different magnetic materials.

second and the third terms respectively denote the interactions between shell spins and those located at the core-shell interface. The last term stands for the Zeeman term. Note that the angular brackets in Eq. (4) represent summations carried out over the nearest neighbor spins whereas the last summation is over all the lattice sites. In order to calculate the magnetic properties, we use Monte Carlo simulation method based on the conventional single-spin update scheme [17, 18]. In order to mimic the finite size of the particle, free boundary conditions were imposed in all directions. Simulations have been carried out over 5000 Monte Carlo steps per spin after discarding 20% for thermalization. We start from a disordered high temperature configuration, and the temperature is gradually decreased down to  $T = 0.01J_c$ . In order to reduce the statistical errors, 10 independent sample realizations were considered at each temperature step. Due to the reduced translational symmetry at the surface we set  $J_s = 0.5J_c$ , and for the interface we also assume a ferromagnetic coupling ( $J_{int} > 0$ ).

In order to study the interfacial effects, the simulated particle is composed of a ferromagnetic core with a varying shape whereas we assume a spherical shell. In this regard, the distance between any spin  $S_i$  and central spin  $S_0$  is given by [19, 20]

$$D_p(S_0, S_1) = (|x_0 - x_1|^p + |y_0 - y_1|^p + |z_0 - z_1|^p)^{1/p}. \quad (5)$$

According to Eq. (5), we can define independent parameters  $p_c$  and  $p_s$  which are called the metric order of the particle core and shell, respectively. Clearly, if the spin-spin distance defined by Eq. (5) with  $p = p_c$  is lower than the core radius then the spin  $S_i$  is assigned to the core part, otherwise it is located at the shell region.

In order to reveal the influence of the interfacial morphology on the magnetic properties, we fix the metric order of the particle shell as  $p_s = 2.0$  which corresponds to a spherical shape in Euclidian geometry. On the other hand, metric order of the particle core is an adjustable parameter which may evolve from asteroid to octahedral, spherical, and cubic shapes with increasing metric order of the

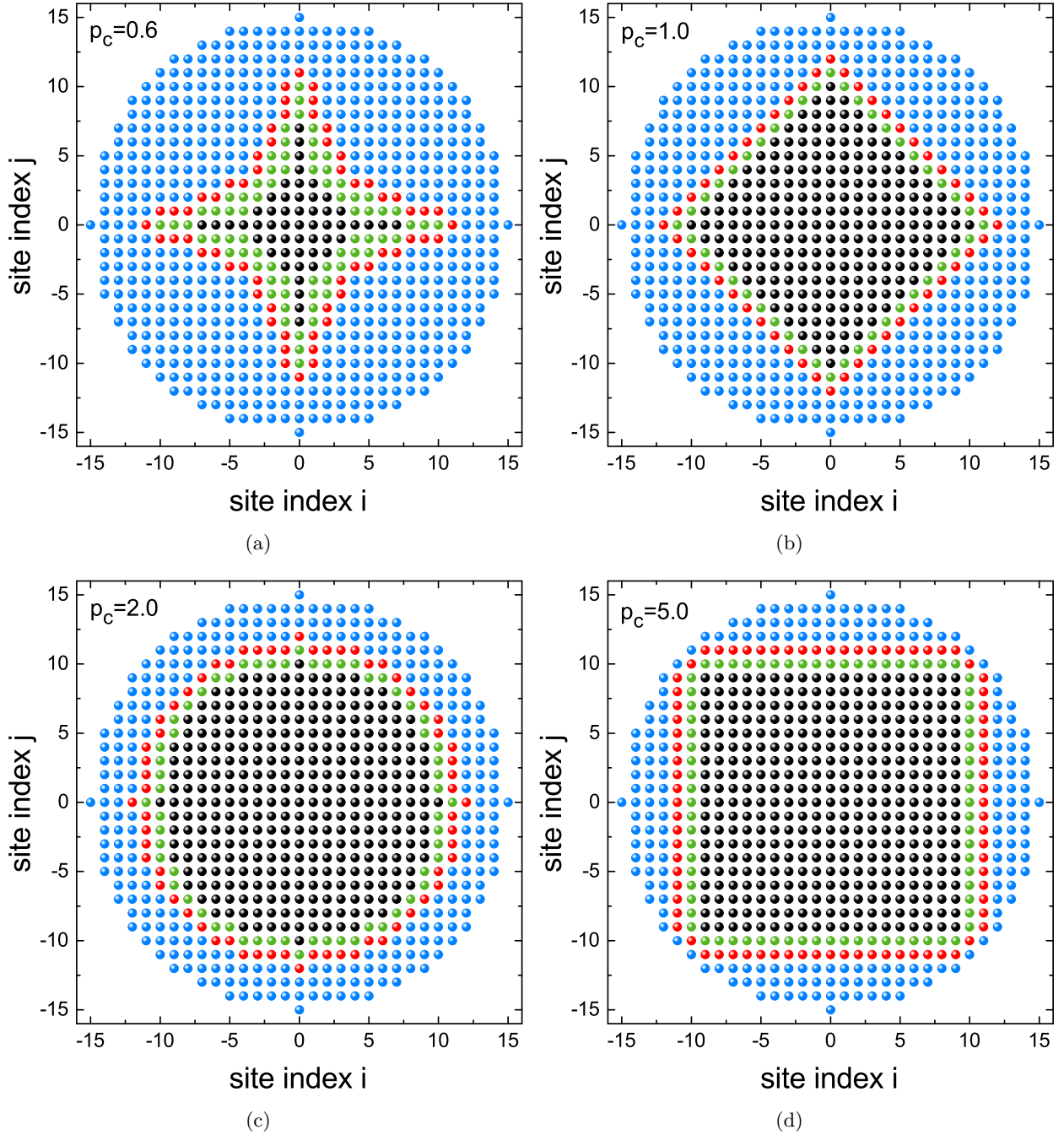


**Figure 2.** 2D cross-sections of the simulated particles with different interface morphology: (a) asteroid, (b) octahedral, (c) spherical, and (d) cubic.

core (cf. Figure 2). In this process, the total particle size and shell thickness values are kept fixed as  $R = 15.0$  and  $R_s = 4.0$  with core radius  $R_c = R - R_s$ , all measured in terms of unitary lattice spacing. Structural properties of the particle, i.e. the variation of the number of lattice sites associated to different parts of the particle are presented in the Appendix (cf. Figure 6).

In addition to the magnetocaloric properties defined in Eqs. (1)–(3), we have also calculated the following magnetic quantities during our simulations:

Thermal averages of the core, shell and total magnetizations are given by

$$M_c = \frac{1}{N_c} \left\langle \sum_{i=1}^{N_c} S_i \right\rangle, \quad M_s = \frac{1}{N_s} \left\langle \sum_{j=1}^{N_s} S_j \right\rangle, \quad M_T = \frac{1}{N_T} \left\langle \sum_{k=1}^{N_T} S_k \right\rangle, \quad (6)$$

where  $N_T = N_c + N_s$  is the total number of spins acting in the system.

Finally, the zero field magnetic susceptibility can be calculated using the relation

$$\chi_T = \frac{1}{k_B T} (\langle M_T^2 \rangle - \langle M_T \rangle^2). \quad (7)$$

In the calculations, we also set  $k_B = 1$  for simplicity.

### 3. Results and discussion

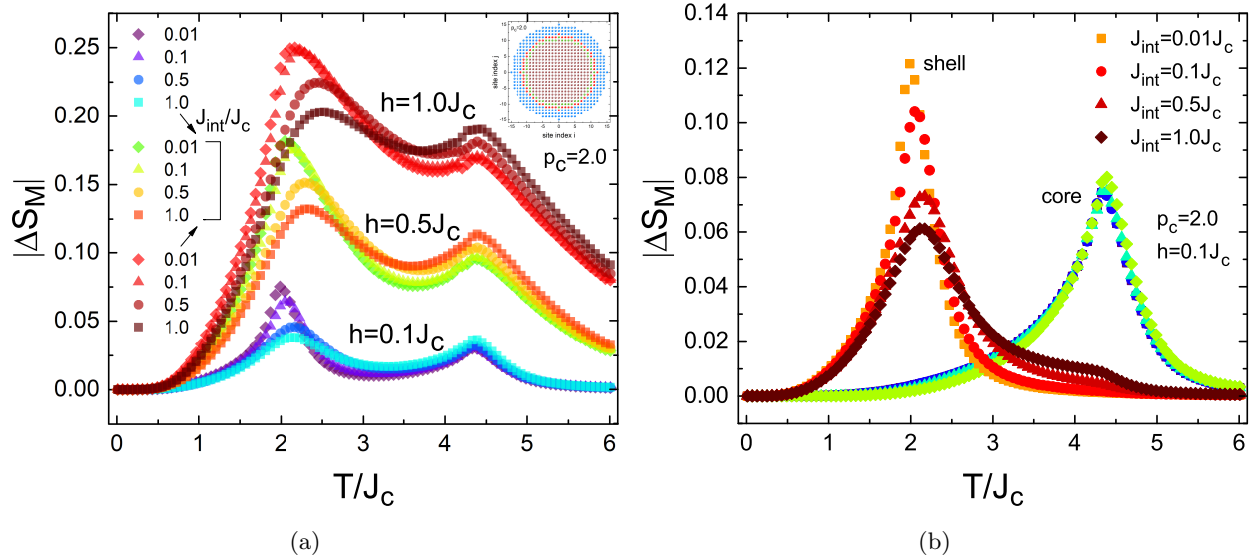


**Figure 3.** Variation of magnetic entropy change of a spherical particle as a function of temperature. (a) Influence of magnetic field on the overall particle is emphasized for  $h = 0.1J_c, 0.5J_c, 1.0J_c$  with a variety of values of the interface coupling  $J_{int}$ . (b) Individual contributions of core and shell parts for a fixed magnetic field strength with a variety of  $J_{int}$  values. Since the curves corresponding to the core contribution overlap with each other, we omit the color codes to avoid any confusion in the figure.

First of all, let us consider a spherical particle with  $p_c = p_s = 2.0$ . As shown in Figure 3a,  $|\Delta S_M|$  versus temperature curves exhibit two maxima. Both maxima of  $\Delta S_M$  curve becomes enhanced with increasing field. This result is well known in the literature. The less known outcome which can be deduced from Figure 3 is that the lower maximum becomes rounded with increasing interface coupling  $J_{int}$  whereas the higher maximum is less affected by increasing  $J_{int}$ . As seen from Figure 3b, lower temperature peak of  $\Delta S_M$  originates as a result of magnetic behavior of the shell

layer whereas the higher temperature peak is associated to the magnetism of the core. As a result of the reduced translational symmetry of the shell layer, the critical behavior of the particle is governed by the core. Hence, with increasing  $J_{int}$ , the shell layer becomes more coupled to the particle core. These results show that multiphase materials may exhibit enhanced magnetocaloric properties such as two characteristic entropy peaks.

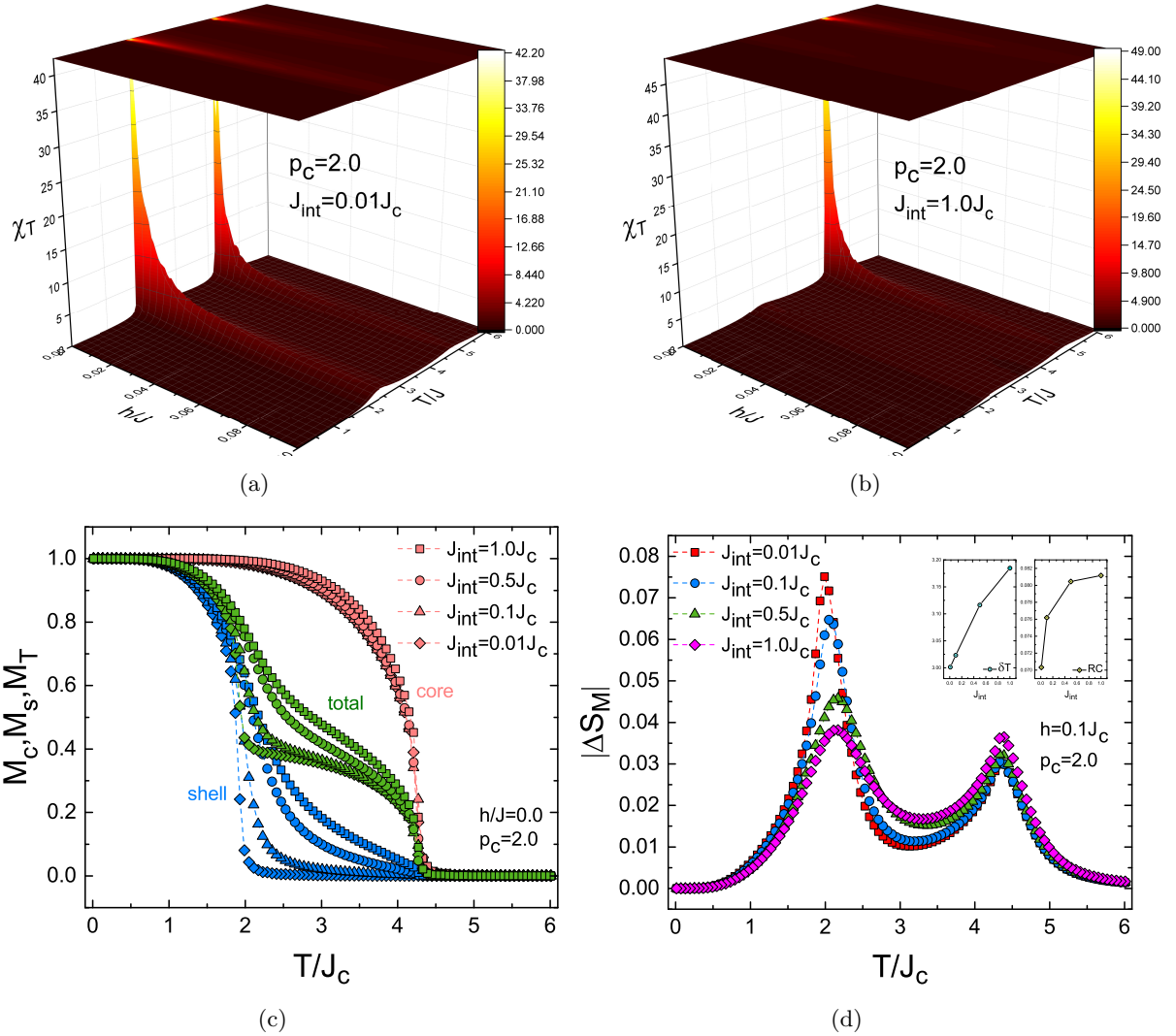


**Figure 4.** (a), (b) magnetic susceptibility, (c) magnetization, (d) magnetic entropy change of a spherical particle. The inset in (d) represents the full width at half maximum and the refrigerant capacity calculated from the entropy curves.

The double peak character also shows itself in the magnetic properties of the particle. In Figure 4, again we consider a spherical nanoparticle model. Figures 4a and 4b show the variation of magnetic susceptibility as a function of magnetic field and temperature for two scenarios, namely, for weak (Figure 4a) and large interface coupling (Figure 4b). For  $J_{int} = 0.01 J_c$ , core and shell parts become independent of each other which manifests itself as two diverging sharp peaks in the temperature



dependence of zero field susceptibility. These sharp peaks quickly become rounded with increasing field. On the other hand, susceptibility behavior corresponding to  $J_{int} = 1.0J_c$  exhibits only one major peak indicating the dominance of the core magnetization against the shell. Similar arguments also hold for the magnetization profiles given in Figure 4c. It is clear that the core magnetization does not depend on the varying interface coupling whereas the shell magnetization is sensitive to varying  $J_{int}$ , as a result of the lack of the translational symmetry of the surface spins. Consequently, low temperature peak of the  $|\Delta S_M|$  curve can be adjusted by properly tuning the interface exchange coupling (Figure 4d). A close inspection of Figures 3b and 4d shows that the low temperature entropy peaks attributed to shell part exhibit a small tendency to shift to higher temperature region with increasing  $J_{int}$  values. The reason is the fact that the thermal variation of the shell magnetization becomes steeper for lower values of  $J_{int}$  (for instance, please see Figure 4c). Consequently, isothermal entropy variation calculated by Eq. (2) exhibits sharp peaks with peak positions shifted to the left for the shell part. As the magnitude of  $J_{int}$  increases, shell magnetization exhibits smooth variation as a function of temperature. Hence, the entropy peaks become broadened and shifted to high temperature region. The inset in Figure 4d shows figures of merit of the MCE, namely the full width at half maximum  $\delta T$  and RC curves, each of which tend to increase with increasing interface coupling. This finding is one of the major results predicted by our simulations: For large values of the interface exchange coupling, the operating temperature interval of the nanocomposite broadens at the expense of the low temperature peak of  $|\Delta S_M|$  which leads to enhanced RC values.

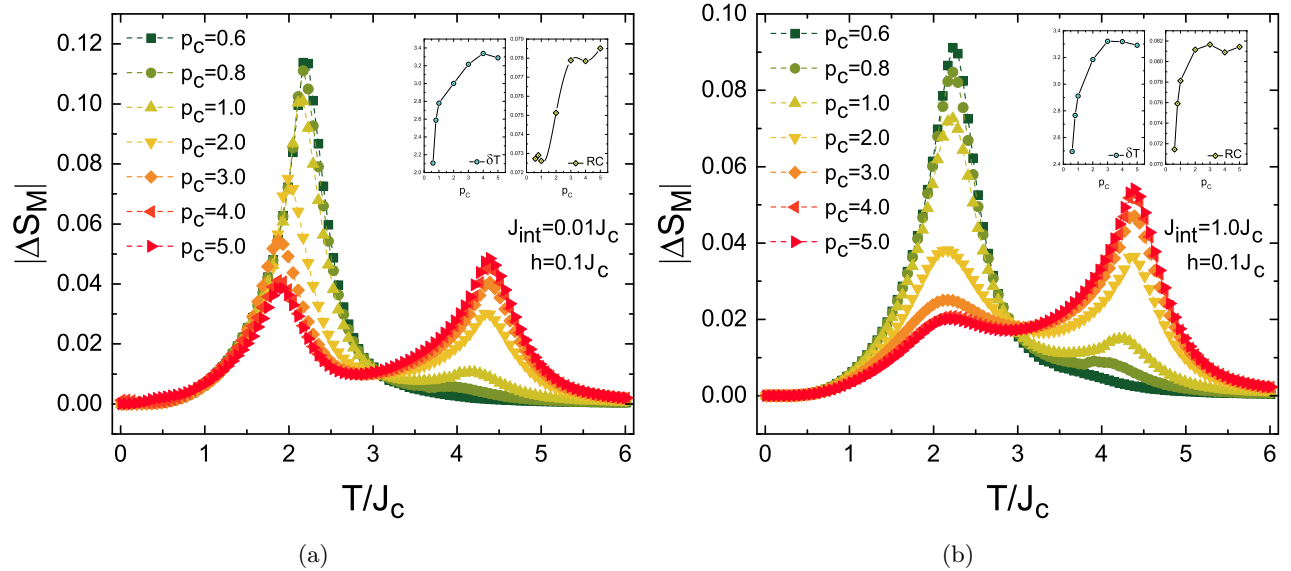


**Figure 5.** Influence of the interface morphology on the thermal variation of total entropy change for (a)  $J_{int} = 0.01J_c$ , (b)  $J_{int} = 1.0J_c$ . Different symbols correspond to different  $p_c$  values. The insets show the full width at half maximum and the refrigerant capacity calculated from the entropy curves.

As our last investigation, in order to see how the shape of the core/shell interface affects the magnetocaloric properties, we monitor the evolution of  $|\Delta S_M|$  versus temperature curves for varying  $p_c$  values. The results are displayed in Figure 5. As the shape of the particle evolves from asteroid to cubic form, the high temperature peak becomes enhanced at the expense of the low temperature maximum. However, the temperature span is enlarged and consequently it leads to an enhancement

of  $\delta T$  and RC values. This behavior holds not only for weak  $J_{int}$  values, but also for large values of the interface exchange coupling. As a result, we conclude that regarding the variation of  $\delta T$  and RC values, MCE properties of the nanocomposites with cubic core are superior to those with the truncated cuboctahedral, spherical, octahedral, and asteroid shaped cores. Besides, it may be possible to adjust the temperature value at which the maximum entropy change occurs which makes the composite material of practical importance for technological applications.

#### 4. Conclusions

In conclusion, we have simulated the magnetic and magnetocaloric properties of a composite nanoparticle system composed of a ferromagnetic core which is surrounded by a ferromagnetic shell. Our results show that;

- The present system may exhibit enhanced magnetocaloric properties in comparison to regular single-phase materials such as the origination of two characteristic entropy peaks.
- In case of a spherical particle, the full width at half maximum and the refrigerant capacity tend to increase with increasing interface coupling.
- For large values of the interface exchange coupling, the operating temperature interval of the nanocomposite broadens at the expense of the low temperature peak of  $|\Delta S_M|$  which leads to enhanced RC values.
- As an interface phenomenon, magnetocaloric properties of the particles with a cubic core are enhanced in comparison with those composed of truncated cuboctahedral, spherical, octahedral, and asteroid shaped cores.

Overall, our results show that it may be possible to fabricate nanocomposite materials with desired refrigerant properties, by manipulating the microscopic details of the interface region of the particle.

We hope that the results presented in this work would stimulate future experimental studies on the exploration of magnetocaloric research.

#### Acknowledgment

The numerical calculations reported in this paper were performed at TÜBİTAK (the Scientific and Technological research Council of Turkey) ULAKBİM (Turkish Academic Network and Information Center), High Performance and Grid Computing Center (TRUBA Resources).



## Appendix

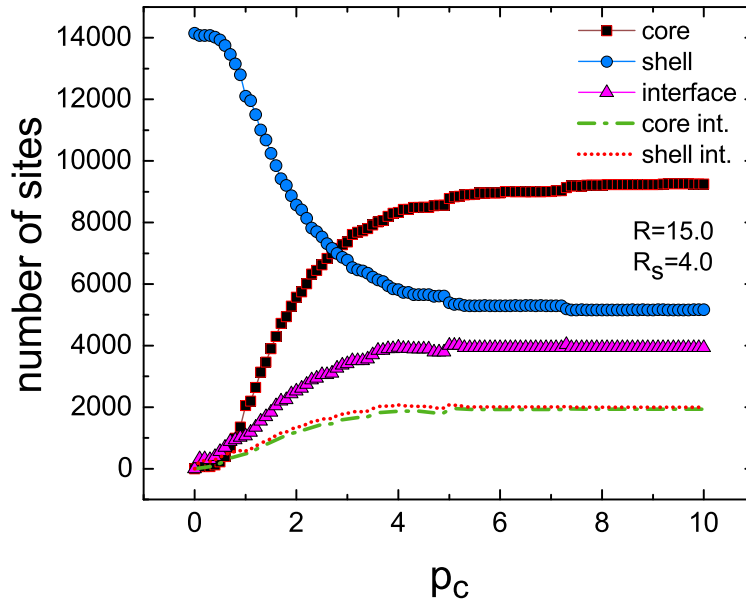


**Figure 6.** Variation of the number of lattice sites belonging to different parts of the modeled nanoparticles as functions of the metric order of the particle core, evolving from asteroid ( $p_c < 1.0$ ) to cube ( $p_c \gg 1.0$ ).

## References

- [1] V. Franco, J. S. Blázquez, B. Ingale and A. Conde, “The Magnetocaloric Effect and Magnetic Refrigeration Near Room Temperature: Materials and Models”, *Annual Review of Materials Research* **42** (2012) 305-342.
- [2] V. K. Pecharsky and K. A. Gschneidner Jr, “Magnetocaloric effect from indirect measurements: Magnetization and heat capacity”, *Journal of Applied Physics* **86** (1999) 565-575.
- [3] K. A. Gschneidner and V. K. Pecharsky, “Magnetocaloric Materials”, *Annual Review of Materials Science* **30** (2000) 387-429.
- [4] V. K. Pecharsky and K. A. Gschneidner Jr, “Advanced magnetocaloric materials: What does the future hold?”, *International Journal of Refrigeration* **29** (2006) 1239-1249.
- [5] N. A. De Oliveira and P. J. Von Ranke, “Theoretical aspects of the magnetocaloric effect”, *Physics Reports* **489** (2010) 89-159.
- [6] X. Q. Zheng, X. P. Shao, J. Chen, Z. Y. Xu, F. X. Hu, J. R. Sun and B. G. Shen, “Giant magnetocaloric effect in  $\text{Ho}_{12}\text{Co}_7$  compound”, *Applied Physics Letters* **102** (2013) 022421-022426.
- [7] R. M'nassri, N. C. Boudjada and A. Cheikhrouhou, “Nearly constant magnetic entropy change involving the enhancement of refrigerant capacity in  $(\text{La}_{0.6}\text{Ba}_{0.2}\text{Sr}_{0.2}\text{MnO}_3)_{1-x}/(\text{Co}_2\text{O}_3)_x$  composite”, *Ceramics International* **42** (2016) 7447-7454.
- [8] X. Q. Zheng, J. W. Xu, S. H. Shao, H. Zhang, J. Y. Zhang, S. G. Wang, Z. Y. Xu, L. C. Wang, J. Chen and B. G. Shen, “Large magnetocaloric effect of NdGa compound due to successive magnetic transitions”, *AIP Advances* **8** (2018) 056425-056430.

- [9] R. Yuan, P. Lu, H. Han, D. Xue and T. Lookman, “Enhanced magnetocaloric performance in manganite bilayers”, *Journal of Applied Physics* **127** (2020) 154102-154109.
- [10] J. Chen, B. G. Shen, Q. Y. Dong, F. X. Hu and J. R. Sun, “Large reversible magnetocaloric effect caused by two successive magnetic transitions in ErGa compound”, *Applied Physics Letters* **95** (2009) 132504-132507.
- [11] X. Q. Zheng, J. Chen, J. Shen, H. Zhang, Z. Y. Xu, W. W. Gao, J. F. Wu, F. X. Hu, J. R. Sun and B. G. Shen, “Large refrigerant capacity of RGa (R=Tb and Dy) compounds”, *Journal of Applied Physics* **111** (2012) 07A917-07A920.
- [12] K. Szalowski and T. Balcerzak, “The influence of interplanar coupling on the entropy and specific heat of the bilayer ferromagnet”, *Thin Solid Films* **534** (2013) 546-552.
- [13] R. Caballero-Flores, V. Franco, A. Conde, K. E. Knipling and M. A. Willard, “Optimization of the refrigerant capacity in multiphase magnetocaloric materials”, *Applied Physics Letters* **98** (2011) 102505-102508.
- [14] V. Franco, A. Conde, D. Sidhaye, B. L. V. Prasad, P. Poddar, S. Srinath, M. H. Phan and H. Srikanth, “Field dependence of the magnetocaloric effect in core-shell nanoparticles”, *Journal of Applied Physics* **107** (2010) 09A902-09A907.
- [15] P. Gorria, J. L. S. Llamazares, P. A. Alonso, M. J. Pérez, J. S. Marcos and J. A. Blanco, “Relative cooling power enhancement in magneto-caloric nanostructured  $\text{Pr}_2\text{Fe}_{17}$ ”, *Journal of Physics D: Applied Physics* **41** (2008) 192003-192008.
- [16] L. E. Hueso, P. Sande, D. R. Miguéns, J. Rivas and F. Rivadulla, “Tuning of the magnetocaloric effect in  $\text{La}_{0.67}\text{Ca}_{0.33}\text{MnO}_{3-\delta}$  nanoparticles synthesized by sol-gel techniques”, *Journal of Applied Physics* **91** (2002) 9943-9947.
- [17] M. E. J Newman and G. T. Barkema, “Monte Carlo Methods in Statistical Physics”, Springer: Berlin, Germany, 1979.
- [18] N. Metropolis, A. W. Rosenbluth, M. N. Rosenbluth, A. H. Teller and E. Teller, “Equation of State Calculations by Fast Computing Machines”, *The Journal of Chemical Physics* **21** (1953) 1087-1092.
- [19] M. Vasilakaki, C. Binns and K. N. Trohidou, “Susceptibility losses in heating of magnetic core/shell nanoparticles for hyperthermia: a Monte Carlo study of shape and size effects”, *Nanoscale* **2015**, 2015, 7753-7762.
- [20] D. Sabogal-Suárez, J. D. Alzate-Cardona and E. Restrepo-Parra, “Influence of the shape on exchange bias in core/shell nanoparticles”, *Journal of Magnetism and Magnetic Materials* **482** (2019) 120-124.